

## Zeeman-Effect Magnetic Field Measurement of a High-Temperature Plasma\*

F. C. JAHODA, F. L. RIBE, AND G. A. SAWYER

*Los Alamos Scientific Laboratory, University of California, Los Alamos, New Mexico*

(Received 14 February 1963)

Distortions of magnetic field measurements caused by material probes in hot plasmas can be avoided by measuring the Zeeman splitting of impurity spectral lines. The problem of the line breadths being large compared to the magnetic field splitting is solved by using the opposite circular polarization characteristics of the symmetrically displaced Zeeman components in a longitudinal field. This, however, limits the technique to wavelengths longer than 2000 Å, where there is a scarcity of intense allowed transitions from the highly ionized species which originate in the hot plasma. Successful measurements have been made on the Scylla I theta pinch device. These indicate approximately zero magnetic field in the hot plasma and set a lower limit of 79% on  $\beta$ , the ratio of plasma to magnetic pressure.

## I. INTRODUCTION

MAGNETIC fields in laboratory plasmas are usually measured with small probes inserted directly into the plasma.<sup>1</sup> These have the advantages of simplicity, high sensitivity, and good spatial resolution. In sufficiently hot plasmas, however, even a ceramic jacket on the probe is eroded, and the consequent cooling of the plasma can lead to gross distortions

of the magnetic field ("breakthrough") which do not occur in the absence of the probe. This fact, which had long been suspected, was recently established with an external, double-probe technique in the case of the Scylla I  $\theta$  pinch.<sup>2</sup> The present experiment was begun before we learned of the successful use of external double probes<sup>3</sup> and was motivated by the desire to study just this field breakthrough induced by probes placed in the Scylla I plasma.<sup>4</sup> This effort was unsuccessful because of the lack of appropriate impurity radiation from the discharge at the time when, in the presence of a plasma probe, the breakthrough occurs. However, the Zeeman-effect measurement technique succeeded and it established the absence of magnetic field (complete plasma diamagnetism) before the breakthrough, giving an independent confirmation of previous plasma probe results.<sup>4</sup> The Zeeman effect technique has a definite advantage over the external double probe because it measures the magnetic field directly. The double probe, on the other hand, is sensitive only to the product of magnetic field and plasma area.

The results as well as the limitations associated with the Zeeman measurement are set forth in detail below in the expectation that the general method can find applicability in other plasma configurations.

## II. PRINCIPLE OF MEASUREMENT

The basic problem with a Zeeman-effect measurement of the spectral-line splitting in a hot plasma arises from the fact that the splitting is invariably small compared to the line breadth. For example, in Scylla I the full value of the external driving field, 50 kG, would give a total separation of the most intense Zeeman components of the C v line at 2271 Å of 0.2 Å, whereas the measured half-width of this line (Fig. 1) is 3.4 Å. Hence, ordinary spectroscopic measurements are incapable of detecting the magnetic field.

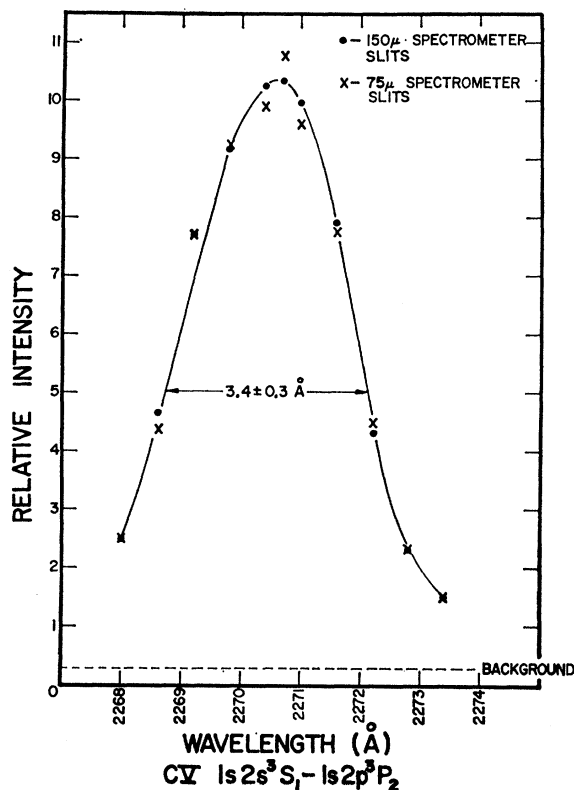


FIG. 1. Measured profile of the short-wavelength component of the C v triplet. The Zeeman-effect measurements were made on the merged long-wavelength components of equivalent total breadth.

\* Work performed under the auspices of the U. S. Atomic Energy Commission.

<sup>1</sup> See, for example, R. H. Lovberg, *Ann. Phys. (N. Y.)* 8, 311 (1959).

<sup>2</sup> F. C. Jahoda and G. A. Sawyer (to be published).

<sup>3</sup> H. A. B. Bodin, T. S. Green, G. B. F. Niblett, N. J. Peacock, J. M. P. Quinn, and J. A. Reynolds, *Suppl. Nucl. Fusion* 2, 511 (1962).

<sup>4</sup> K. Boyer, W. C. Elmore, E. M. Little, W. E. Quinn, and J. L. Tuck, *Phys. Rev.* 119, 831 (1960).

An elegant solution has been highly developed by Babcock<sup>5</sup> to overcome the same problem in measuring solar magnetic fields. It utilizes the opposite circular polarizations of the symmetrically displaced Zeeman components in a longitudinal field. Figure 2 illustrates the idea. It represents the intensity distribution as a function of wavelength separately for the two circular polarization components for the case of line breadth large compared to the separation. If the two polarization components can be detected separately off the line center, then their relative intensity is a function of the magnetic field.

In the astrophysical case two symmetrically located slits are used and the polarizations are examined alternately by 60-cps modulation of a quarter-wave plate. Photoelectric recording of the modulated difference signal between the two slits permits field measurements routinely down to field strengths which give a splitting of only one part in  $10^4$  of the line breadth.

Most laboratory plasmas, however, are of a transient variety ( $\sim 0.5 \mu\text{sec}$  for Scylla I) and not readily amenable to modulation techniques. In this case both polarizations must be measured simultaneously with pulse techniques and this entails a great loss of sensitivity. Furthermore, to eliminate nonmagnetic time-dependent effects it is desirable to measure both components at the same wavelength (one slit). For example, total line intensity variations for two imperfectly symmetric slits or Stark shifts resulting from electric fields would give spurious intensity differences between two different wavelengths. The experimental arrangement, outlined below, which achieves simultaneous observations of both polarizations at the same wavelength, necessitates strong line intensity. This, however, is not as restrictive as appears at first sight, since the line radiation must in any case be sufficiently strong to stand out well above the plasma continuum radiation.<sup>6</sup>

An even more basic limitation on the laboratory plasma measurement, of little consequence to most of the astrophysical applications, is the fact that the need for polarization optics limits one to using wavelengths above the practical transmission limit of crystal quartz, at about 2000 Å. There is an almost complete absence of strong lines above this wavelength from species sufficiently ionized so that the radiation originates in the hot plasma core that one wishes to examine. In the present case the plasma has an electron temperature of 350 eV.<sup>7</sup> On the other hand, long wavelengths are advantageous because the magnetic field splitting, proportional to wavelength squared, becomes a larger fraction of the line breadth, which is dominated by Doppler broadening and directly proportional to wavelength.

<sup>5</sup> H. W. Babcock, *Astrophys. J.* **118**, 387 (1953); *Sci. Am.* **202**, 53 (February 1960).

<sup>6</sup> F. C. Jahoda, E. M. Little, W. E. Quinn, G. A. Sawyer, and T. F. Stratton, *Phys. Rev.* **119**, 843 (1960).

<sup>7</sup> A. J. Bearden, F. L. Ribe, G. A. Sawyer, and T. F. Stratton, *Phys. Rev. Letters* **6**, 257 (1961).

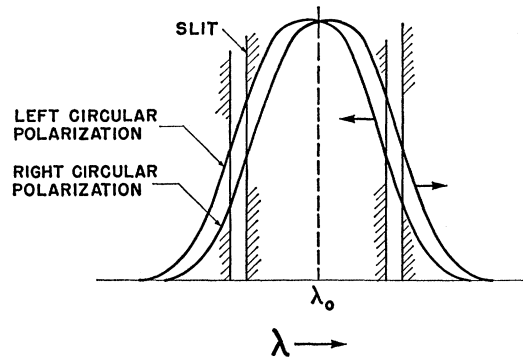


FIG. 2. Intensity vs wavelength for the two circular polarization components of a broadened spectral line split by a longitudinal magnetic field.

For deuterium plasmas, appropriate impurities must be used to obtain suitable spectral lines. If these are introduced in gaseous form before the initiation of the discharge, they participate in all phases of the plasma heating and dynamics. In normal Scylla I operation there is about 2% oxygen impurity naturally present<sup>6</sup> and additional impurities up to 10% concentration do not greatly affect the basic operation. The effect of impurities can be monitored by electron temperature<sup>7</sup> and neutron production. However, there exist cases<sup>8</sup> where the controlled introduction of impurities qualitatively changes the plasma behavior, just as the introduction of material probes does, so that the Zeeman-effect measurement, too, would give rise to spurious magnetic field distortions.

### III. EXPERIMENTAL ARRANGEMENT

The radiation originates in the plasma formed during the second half cycle of the magnetic field of the single-

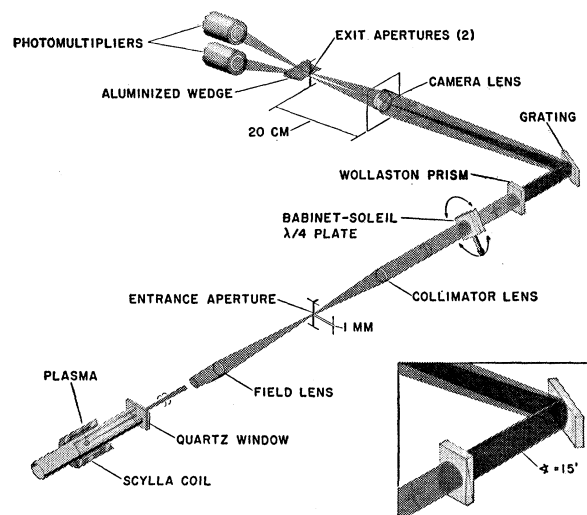


FIG. 3. Schematic diagram of experimental arrangement.

<sup>8</sup> P. Bogen, E. Hintz, and J. Schlüter, *Bull. Am. Phys. Soc.* **8**, 148 (1963).

turn compression coil in the Scylla I  $\theta$  pinch. The damped sinusoidal magnetic compression field has a half period of  $2.5 \mu\text{sec}$  and a peak value during the second half cycle of 50 kG. Previous experiments<sup>4,6</sup> have shown that the radiation from ions of high excitation potential originates in a central region having a diameter of approximately 1.5 cm and an approximate length of 2 cm. The plasma electron density is  $5 \times 10^{16} \text{ cm}^{-3}$ .

Figure 3 is a schematic diagram of the experimental apparatus. Plasma radiation containing both circular polarization components is imaged on the front slit of the monochromator. The slit height is restricted to less than 1 mm. After the light is made parallel by the collimator lens (quartz and fluorite elements are used throughout the optical system) it passes through a tunable quarter-wave plate (Babinet-Soleil compensator) from which the two circular polarizations emerge as mutually perpendicular linear polarizations in spatial directions fixed by the orientation of the optic axis of the quarter-wave plate. A Wollaston prism, with its optic axis appropriately aligned with respect to that

TABLE I. Basic data on spectral transitions used. The number in parentheses in the last column is the ionization potential of the next lower ionization state.

Spectrum	Transition	Wave-length (Å)	$g$ factor	Excitation potential (eV)	
C v	$1s2s \ ^3S_1 - 1s2p \ ^3P_{1,0}$	2277.9 2277.3	1.8	304	(64)
B iv	$1s2s \ ^3S_1 - 1s2p \ ^3P_1$	2826.7	1.75	203	(38)
C iii	$2s2p \ ^1P_1 - 2p^2 \ ^1D_2$	2296.9	1	18	(24)
O v	$2s3s \ ^3S_1 - 2s3p \ ^3P_1$	2787.9	1.75	67	(77)
Cd i	$5s^2 \ ^1S_0 - 5s5p \ ^1P_1$	2288.0	$\sim 1$	5.4	

of the quarter-wave plate, separates the two linear polarizations into two beams diverging at an angle of  $\sim 15$  min of arc in a plane parallel to the rulings of the grating, so that the beams have equal angles of incidence on the grating. After dispersion, monochromatic light is refocused on the exit slit, where two nonoverlapping images of the entrance aperture are formed along the slit dimension. The aluminized wedge enables these to be separately recorded by two photomultipliers. The two images consist of what was originally only right and left circular polarization, respectively.

By rotating the quarter-wave plate through  $90^\circ$  between discharges the Zeeman components corresponding to the signals which finally appear in the photomultipliers are interchanged. Normalizing the two ratios of the signals thus obtained eliminates the effect of relative gain differences in the two channels. However, slight displacement of the image along the direction of dispersion when the quarter-wave plate is rotated would produce spurious intensity differences when the slit is located on the wing of a steep line

profile. Proof that this effect is negligible is the observation of an equal magnetic signal but of opposite polarity on the opposite wing of the line profile.

The grating is a 1200 lines/mm Bausch and Lomb replica, blazed for  $1 \mu$ . Generally, it was used in 4th order, with a  $100 \text{ \AA}$  bandpass interference filter in front of the entrance slit to eliminate other orders. Linear reciprocal dispersion at the exit slit is approximately  $10 \text{ \AA}/\text{mm}$ . Data were mostly obtained with  $150\text{-}\mu$  entrance and exit slits.

A slight complication, not indicated in Fig. 3, is the fact that the grating efficiency for the two linear polarizations, necessarily parallel and perpendicular, respectively, to the grating rulings, is very different. The relative efficiency is a strong function of wavelength and was found to vary by a whole order of magnitude. In order not to lose signal intensity unnecessarily by reducing the gain in the more efficient channel, a crystal quartz plate cut perpendicular to the optic axis and of appropriate thickness for rotating both beams to make an angle of  $45^\circ$  with the grating rulings was inserted after the Wollaston prism.

#### IV. SPECTRAL LINES

Table I lists several spectral lines used for Zeeman effect measurements. Almost unique in satisfying the requirements of long wavelength, high intensity, and large excitation potential is the triplet  $2s-2p$  transition of C v, a member of the He I isoelectronic sequence. The two unresolved long-wavelength components are listed because their larger effective  $g$  value relative to the  $J=2$  component increases the magnetic field splitting. This transition has high intensity even though the lower energy level is not the ground state because there are no levels below it to which allowed optical transitions from the upper level can occur. The next lower member of this isoelectronic sequence, B iv, is at longer wavelength but its excitation potential is a hundred eV less. Not listed is the next higher member, N vi, which falls at  $1898 \text{ \AA}$ . While its measurement is still possible in principle, this wavelength has an additional attenuation factor of 30 in the optical elements, leading to excessive noise problems.

The C iii transition at almost the same wavelength as C v and of relatively low excitation potential is intrinsically bright for the same reason that C v is bright. It is also excited in the Scylla discharge and is particularly useful as an instrumental calibration.

The O v transition, again meeting the criterion for high intensity, is of intermediate excitation potential and at a wavelength close to that of B iv. The Cd i resonance line, lying between the two carbon lines in wavelength, is included because it was used to demonstrate the greater dc sensitivity of the instrument. Also, since the lenses are not perfect achromats over large wavelength ranges, this line was extensively used in the alignment procedure.

## V. EXPERIMENTAL RESULTS

The sensitivity with which magnetic fields,  $B$ , can be measured depends on the square of the wavelength,  $\lambda$ , the Landé  $g$  factor, and the slope of the line profile,  $s$ . Assuming for the small displacements involved that the line intensity is a linear function of distance along the direction of dispersion, the relative intensity changes at the exit slit for the two oppositely displaced components are

$$(I \pm \Delta I)/I = 1 \pm k\lambda^2gsB, \quad (1)$$

respectively, where  $k$  is a constant. In principle,  $k$  can be evaluated from the Zeeman-effect theory, but in practice this was always found to considerably overestimate the relative intensity change. The reason for this is that transverse fields, continuum radiation, slight misalignments, and the apparatus window function all tend to degrade the observed effect. The procedure adopted was to make a measurement in a known field strength  $B_0$ , at a reference wavelength  $\lambda_0$ , and, thus, empirically to determine  $k$ .

Each simultaneous measurement of both polarizations yields a ratio

$$R = (1 + k\lambda^2gsB)/(1 - k\lambda^2gsB), \quad (2)$$

if the gains of the two channels are equal. As already indicated, for the Scylla measurements, instead of keeping perfectly matched gains, two ratios were always obtained on separate discharges, with the quarter-wave plate rotated to interchange beam identity, and the term ratio, henceforth, refers to the geometric mean of the two ratios thus obtained. The convention is adopted always to express the ratio as a number greater than unity, and to prefix it with an algebraic sign according to which quarter-wave plate position gives the larger signal in one particular channel. The polarity of the measured field is given by the algebraic sign, taking into account whether the measurement is made on the short- or long-wavelength side of the line.

Finally, bearing in mind that  $k\lambda^2gsB \ll 1$ , Eq. (2) can be used to get the following relation for an unknown magnetic field in terms of the reference field:

$$B \approx B_0 \frac{\lambda_0^2 g_0 s_0 (|R| - 1)}{\lambda^2 g s (|R_0| - 1)}, \quad (3)$$

where the subscripts refer to the reference case, which may or may not use the same spectral line.

Figure 4 shows some sample data. These dual oscilloscope traces are the outputs of the two photomultipliers for the two positions of the quarter-wave plate at exit slit positions on the long-wavelength wings of C v and C III, respectively. These were obtained

with 10% methane added to the deuterium gas. The signals have been smoothed by a 2-Mc/sec cutoff low pass filter, which also introduces some phase shift. This, however, has been compensated for by the positioning along the time axis of the external compression field trace (using data obtained without the low pass filter). It can be seen that the C v light peaks and decays before the peak of the second half-cycle. It is also apparent that the C v traces show very little relative difference in either quarter-wave plate position. However, for the C III case, at the first peak (first half-cycle) the upper beam has a larger signal relative to the lower beam in the  $-45^\circ$  position, while for the late C III peak (second half-cycle) this occurs in the  $+45^\circ$  position. This consistent feature results from the fact that the external driving magnetic field reverses polarity between the half-cycles and convincingly demonstrates that the gross relative intensity variations (above noise fluctuations) are magnetic field effects.

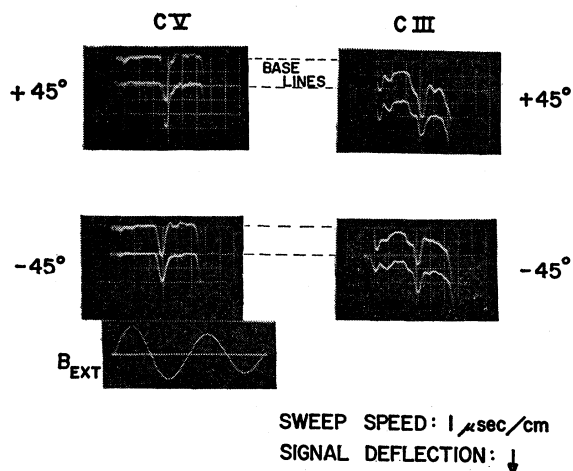


FIG. 4. Oscilloscope traces showing the separate photomultiplier signals resulting from the two positions ( $+45^\circ$  and  $-45^\circ$ ) of the quarter-wave plate. The slit of the spectrometer was on the long-wavelength wings of the C v and C III lines. The oscillogram of the compression field  $B_{ext}$  establishes the time of occurrence of the light signals.

It is not shown in Fig. 4, but it was verified by experiment that the relative polarities reverse on the low-wavelength wing of the line profile.

The fact that the pairs of traces in Fig. 4 do not have quite identical shapes indicates that the noise level is not negligible. This noise is predominantly shot noise in the photomultipliers, and for the peak amplitudes observed is calculated to be  $\sim 8\%$  of the signal. Since this, in turn, is not negligible relative to the intensity differences to be measured, it was necessary to collect statistics on many pairs ( $\sim 30$ ) of oscilloscope traces. The quantitative results are given in Table II. The indicated errors on the intensity ratios are the standard deviations of the mean values. These are the main contributions to the cumulative errors which give

TABLE II. Quantitative results of the analysis of several sets of oscilloscope traces of the kind shown in Fig. 4.

Half cycle	Spectral line	Normalized slope ( $\pm 10\%$ )	$g$ factor	Intensity ratio	$B_{\text{external}}$	$B_{\text{plasma}}$	$\beta^a$
1st	C III (2296 Å)	1	1	+1.11 $\pm$ 0.02	+27.5 kG	+27.5 kG <sup>b</sup>	0
2nd	C III (2296 Å)	0.69	1	-1.10 $\pm$ 0.02	+38.5	-37 $\pm$ 6	< 0.36
2nd	C V (2278 Å)	0.32	1.8	+1.006 $\pm$ 0.009	-28.5	+ 3 $\pm$ 10	> 0.79

<sup>a</sup>  $\beta = 1 - (B_{\text{plasma}}^2/B_{\text{external}}^2)$ .

<sup>b</sup> Set equal to  $B_{\text{external}}$  as a calibration.

the range of uncertainty in the plasma magnetic field results.

The third column from the right in Table II lists the value of the applied external magnetic field at the instant when the given line has its peak intensity. During the first half-cycle of the discharge the plasma temperature is known to be low (not more than a few eV), and it shows no hydromagnetic properties characteristic of the second half-cycle.<sup>4,6</sup> Plasma probes show that the driving magnetic field completely penetrates the plasma during the first half-cycle.<sup>2,4</sup> This allows the C III signal during the first half-cycle (first line, Table II) to be used as a calibration, since its magnetic field value can be set equal to the known external field. The magnetic fields corresponding to the intensity peaks during the second half-cycle are then computed according to Eq. (3).

During the second half-cycle the C III line, being easily excited, should originate only in the outer, cooler regions of the plasma, near the interface between the plasma and the external magnetic field. This is borne out by the results of the second line of Table II, which show that the plasma  $B$  value indicated by C III during the second half-cycle is approximately equal to that of the driving field and has the same polarity. The C V line, however, originates in the hot plasma core and its corresponding  $B$  value (third line, Table II) is approximately zero. The data indicate a small reversed field which, within experimental error, cannot be distinguished from zero, in agreement with the result of plasma probes before the peak of the second half-cycle.

The last column of Table II lists bounds on  $\beta$ , the ratio of particle to magnetic pressure during the second half-cycle at the places in the plasma from which the C III and C V radiations originate. The C V data show a value of  $\beta$  greater than 79% for the hot-plasma core. If, on the other hand, this experiment is regarded as validating the plasma probe measurements before the breakthrough, more precise values of  $\beta$  can be assigned. In particular, the experiment supports the probe result that Scylla I creates a  $\beta \approx 1$  plasma.

As already indicated, the C V light, which has the highest excitation potential of any usable line, decays (i.e., practically all the carbon impurity is ionized to C VI) before the peak of the second half-cycle when the field breakthrough, now known to be caused by the

presence of a plasma probe, occurs. It was observed that the more easily excited species, O V and B IV, which were also "burned through" before the time of peak field, had a second maximum during the cooling phase after peak compression. If these late peaks had given zero-field results in the absence of a probe, this experiment would also have demonstrated the dependence of the breakthrough on the presence of a plasma probe. While this did not occur, the results are briefly summarized below, since they both confirm the C V result already discussed and illustrate a possible pitfall to be avoided in the interpretation of results.

The O V line gave a result that scales according to Eq. (3), again with C III as a reference, to  $-20 \pm 6$  kG for both of its intensity maxima, before and after peak compression. This line of intermediate excitation potential apparently originates not in the plasma core nor as far out as C III, since it shows a substantial fraction of the external field. It is, therefore, not a sensitive indicator of whether or not a collapse of a small diamagnetic core (the probe breakthrough) occurs.

The B IV line was excited by adding diborane ( $B_2H_6$ ) to the discharge. Despite the fact that its transition probability<sup>9</sup> is very close to that of C V its intensity was very much less, and, in particular, the second peak was subject to very large fluctuations between discharges in an uncontrollable manner. This unexplained behavior itself urges caution in interpreting the results obtained with this line. These agreed with the zero field result of C V for the intensity maximum before peak compression and showed a very large field ( $\sim 45$  kG) of the external field polarity for the second intensity maximum after peak compression. In view of the fact that the plasma core is now known to remain diamagnetic in the absence of a probe,<sup>2</sup> it is concluded that this late B IV light originates very near the outer plasma boundary. The importance of determining where in space the line being examined for Zeeman effect is predominantly excited is obvious.

Despite the statistical data analysis the error limits on measured field magnitudes are fairly large. This was not considered too serious for the original objective of determining whether or not a field breakthrough ( $\sim 50$  kG) occurs. However, for measuring field magnitudes larger signal-to-noise ratios would be desirable.

<sup>9</sup> M. G. Veselov, Zh. Eksperim. i Teor. Fiz. 19, 959 (1949).

In order to demonstrate the system capability a dc measurement was made on the cadmium resonance line with the source placed between the pole pieces of a 2-kG Alnico permanent magnet. A hole was bored through the magnet that permitted longitudinal field observations. The slope of the line profile, normalized as in Table II, is 2.1. The combination of steep slope, and pen recorder output to average over residual noise, gave an easily observed 2% modulation when the quarter-wave plate was manually rotated. Again, opposite polarities were indicated on the opposite line wings. The limitation in accuracy here was a modulation of equivalent magnitude in the absence of the magnet, resulting from slight image displacements when the quarter-wave plate was rotated, which was subtracted out for the field measurement.

### CONCLUSION

The Zeeman effect technique has been successfully applied to measuring transient plasma magnetic fields within rather large uncertainty limits. It has been established that a nearly completely diamagnetic plasma is produced in the Scylla theta pinch device. The basic limitation on the method is the scarcity of spectral lines at wavelengths above 2000 Å which have sufficiently high excitation potentials to be emitted from the hot central region.

### ACKNOWLEDGMENTS

It is a pleasure to acknowledge the technical assistance at various times of W. P. Basmann, W. H. Borkenhagen, A. T. Brousseau, I. Henins, and R. D. Hicks.

## Experimental Test for the Dynamo Theory of Earth and Stellar Magnetism\*

F. WINTERBERG

Case Institute of Technology, Cleveland, Ohio

(Received 4 February 1963)

The dynamo theories to explain earth and stellar magnetism are confronted with great theoretical difficulties. For this reason it has not been possible to reach a final conclusion on the feasibility of self-sustaining hydromagnetic dynamos. In order to solve these difficulties, it is suggested to test the dynamo theory experimentally under laboratory conditions. It is proposed to put a liquid conductor into a container of a rapidly rotating ultracentrifuge. To "drive" the dynamo, forceful fluid motions must be induced in the liquid conductor. This can be done either by externally applied forces, for instance by propellers, or by thermal convection. By assuming the validity of similarity laws it is possible to show that conditions presumably present in stellar-size dynamos can be simulated under laboratory conditions.

### INTRODUCTION

IT is still an unsolved question how magnetic fields can arise in the earth and stars.

Permanent magnetic fields to explain earth or stellar magnetism must be excluded because of the high temperatures involved. Thermoelectric effects have been considered for the earth but are certainly in stars completely insufficient to give anything comparable with the observation. On the other hand, it is a well-known fact<sup>1</sup> that the time for the Ohmic dissipation of a stellar magnetic field is of the order of  $10^{11}$  yr, assuming a uniform star possessing a magnetic field being dipole-like outside the star. As a consequence of this long time scale, the origin of the stellar magnetic field must be sought at the birth of the star or at an even earlier time.

On the other hand, it is very likely that turbulent convection within a star will eventually destroy a magnetic field in a much shorter time than  $10^{11}$  yr. If

this is the case, some kind of regenerative mechanism is necessary to explain stellar magnetic fields.

The only reasonable answer to this problem seems to be the hydromagnetic dynamo.<sup>2</sup> Different models for such dynamos have been proposed but no final conclusion has been reached. For an account of these efforts, together with the references, see for instance Cowling.<sup>3</sup>

### 1. FORMULATION OF THE PROBLEM

We start with the well-known equations of magneto-fluid dynamics.<sup>4</sup>

1. Navier-Stokes equation:

$$\frac{\partial \mathbf{v}}{\partial t} + (\mathbf{v} \cdot \text{grad}) \mathbf{v} = -\frac{1}{\rho} \text{grad } p - \frac{1}{4\pi\rho} \mathbf{H} \times \text{curl } \mathbf{H} + \frac{\eta}{\rho} \nabla^2 \mathbf{v} + \frac{1}{\rho} \left( \zeta + \frac{1}{3} \eta \right) \text{grad } \text{div } \mathbf{v} + \frac{\mathbf{f}}{\rho}. \quad (1.1)$$

<sup>2</sup> J. Larmor, Brit. Assoc. Advance Sci. Rept. **1919**, 159 (1919).

<sup>3</sup> T. G. Cowling, *Magnetohydrodynamics* (Interscience Publishers, Inc., New York, 1957).

<sup>4</sup> For instance, L. D. Landau and E. M. Lifshitz, *Electrodynamics of Continuous Media* (Pergamon Press, Inc., New York, 1960), p. 213 ff.

\* Supported in part by the National Aeronautics and Space Administration.

<sup>1</sup> W. M. Elsasser, Phys. Rev., **69**, 106 (1946).

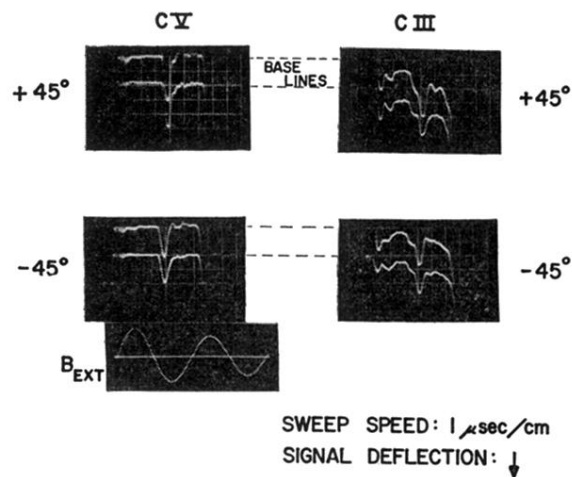


FIG. 4. Oscilloscope traces showing the separate photomultiplier signals resulting from the two positions ( $+45^\circ$  and  $-45^\circ$ ) of the quarter-wave plate. The slit of the spectrometer was on the long-wavelength wings of the C v and C III lines. The oscillogram of the compression field  $B_{\text{ext}}$  establishes the time of occurrence of the light signals.